

RTU
ZINĀTNISKIE
RAKSTI

SCIENTIFIC
PROCEEDINGS
OF RIGA
TECHNICAL
UNIVERSITY



A RHITEKTŪRA UN BŪVZINĀTNE

A R C H I T E C T U R E
A N D C O N S T R U C T I O N S C I E N C E

SĒRIJA 2
SĒJUMS 2

RĪGA 2001



BŪVZINĀTNE

	<i>Belindževa-Korkla O.</i> Ēku ietekmes uz vidi novērtēšanas sistēmas	87
	<i>Brauns J., Rocēns K.</i> Mitrumjūtīgu slāņainu materiālu projektēšana dažādas nozīmes pielietošanai	96
10	<i>Jeļisejevs B.</i> Ķīmisko pretslīdes reagentu salīdzinošā analīze	108
16	<i>Lapsa V.A.</i> Strukturēti ēku siltuma izolācijas un nesoši būvmateriāli.....	116
22	<i>Neilands R., Gjunsburgs B.</i> Izskalojumu attīstība tiltu balstu vietās līdzenuma tipa upēs	132
35	<i>Pakrastiņš L., Rocēns K.</i> Hierarhiskie vanšu pārsegumi	130
2	<i>Rikards R., Korjakins A., Ivaškova A.</i> Plūsuma kritēriju izstrāde kompozītiem, pielietojot kompakto stiepes-bīdes paraugu	136
9	<i>Rikards R., Korjakins A., Kovalevs A., Čate A.</i> Vispārējo materiāla īpašību noteikšana izmantojot neliela izmēra paraugus	147
5	<i>Rubulis J., Sprogis J.</i> Ūdens patēriņa uzskaitē Rīgas pilsētas dzīvokļos	161
1	<i>Serdjuks D., Rocēns K.</i> Sedlveida vanšu pārseguma ar padevīgu savilci racionālā forma	165
	<i>Skudra A.M., Skudra A.A., Krūkliņš A.A.</i> Ar ārēji piestiprinātām stiegotu plastiku sloksnēm pastiprinātas nesaplaisājušas dzelzsbetona sijas spriegumstāvoklis	171
	<i>Šahmenko G.</i> Betonu sastāvu projektēšana ar granulācijas metodi	181
	<i>Zariņš A., Naudžuns J.</i> Ceļa trases projekta līnijas aprakstam lietoto funkciju analīze	191
	<i>Straupe V. Naudžins J.</i> Mazāko kvadrātu metodes pielietojums satiksmes intensitātes izmaiņu analīzei....	195

CHARACTERIZATION OF MATERIAL PROPERTIES BY MEANS OF SMALL SPECIMENS

Rikards R., Korjakins A., Kovalevs A., Čate A.

laminated composites, material properties, identification method

Introduction

Over the past decades several non-metallic, high strength, lightweight fiber reinforced plastics, primarily developed for aerospace and defense application, have been successfully used in the building engineering. A worldwide interest is being given to the use of fiber reinforced plastic materials in bridge structures [1, 2]. There are three kinds of the commercially available fibers: glass, aramid and carbon. Fiber reinforced plastic can be formed into rods, grids, sheets and winding strands. Recent research and experiments related to the use of composite material for repair existing bridges have shown that this method is more cost-effective and requires less effort and time than traditional methods. Composite materials offer unique advantages in solving many practical problems in areas where conventional materials fail to provide satisfactory service life [3]. Unlike steel, composites are claimed to have better corrosion-resistant properties. The first problem connected with using Carbon Fiber Reinforcing Plastics (CFRP) for bridge repair and rehabilitation is characterization of material properties. In this paper the material properties of unidirectional CFRP have been determined using ASTM recommendations.

The aim of the work is to obtain mechanical properties of unidirectional carbon/epoxy composite material. The plates from this material have been manufactured by Israel Aircraft Industries Ltd. Plates have sizes in plan 200*200 mm*mm and four kind of thickness: 1.0 mm, 2.0 mm, 2.16 mm and 6.0 mm.

The static tests for the definition of material properties were performed according ASTM guidelines.

2 Experimental equipment

The tests were performed at the Riga Technical University, using MTS and Hottinger testing system. The wedges type grips have been used for tension test.

2.1 Testing machine

The testing machine is a MTS static testing system Model 809.40. The machine parameters allow a total displacement 500 mm. Maximal vertical load is equal to 500 kN. The mechanical grips clamp the specimens so to minimise the bending strains. A detail of the MTS testing machine with a specimen ready for a tension test and a dummy specimen are shown in Fig. 1.

2.2 Strain gauges

Strain gauges are installed on the surfaces of the specimens, in accordance with ASTM guidelines and glue instruction. The used strain gauges КФ 5П1-5-100-Б-12 are manufactured in Russia. The nominal resistance is equal to 100 Ohm $\pm 0.5\%$ and the gauge factor is equal to $2.19 \pm 1\%$. They present low transverse sensitivity that is equal to $\pm 0.2\%$, and low influence of the temperature on the gauge factor, that is about $0.0001/C^\circ$ between $-10^\circ C$ and $+50^\circ C$.

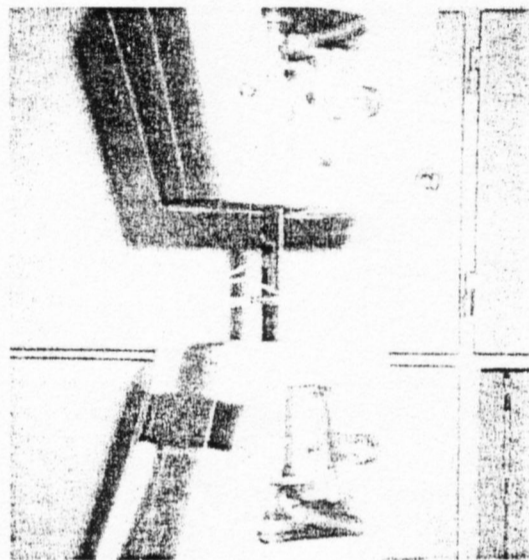


Fig. 1 Tension test.

3 Characterization tests

The following tests, according to the ASTM, are accomplished for the definition the mechanical properties:

1. TEN11 - determination of the tensile strength and tensile modulus at 0° fibre alignment and in-plane major Poisson's ratio
2. TEN22 - determination of the tensile strength and tensile modulus at 90° fibre alignment and in-plane minor Poisson's ratio
3. TEN12 - determination of the shear modulus
4. COM11 - determination of the compression strength and compression modulus at 0° fibre alignment
5. COM22 - determination of the compression strength and compression modulus at 90° fibre alignment
6. COM12 - determination of the shear strength
7. SHR11 - determination of the interlaminar shear strength

Six specimens are tested for each group of tests.

3.1 TEN11 test

Test TEN11 is performed for determination of the tensile strength and the tensile modulus at 0° fibre alignment according with ASTM D3039-76. The specimen lay up consists of 16 plies at 0°. The total thickness is equal 2.0 mm and width of specimen is equal 12 mm with consequently cross sectional area $A=24.0 \text{ mm}^2$. The specimens are 200 mm long and have brackets at the ends with thickness 1.5 mm and length 60.0 mm

Two strain gauges are applied - one in the longitudinal direction and second in the transverse direction.

The tensile modulus is at first calculated using a linear regression of the longitudinal stress-strain curve and then according to the equation

$$E_1^t = \frac{\Delta P}{A \Delta \epsilon}$$

where ΔP is the load difference at the beginning and end of straight line part of stress-strain curve, $\Delta \epsilon$ is a difference between strains at the same part of curve and A is the specimen cross section area.

The Poisson's ratio is obtained as ratio between transverse and longitudinal strains. The tensile strength is calculated as ratio of the ultimate tensile load to the specimen cross sectional area.

The mean values of the tensile modulus, the Poisson's ratio and the tensile strength are presented in Table 1. Also the standard deviations are shown.

Table 1. The mean values for the test TEN11

	Mean value	Standard deviation, %
Tensile modulus E_{11}^t , GPa	176.0	1.85
Poisson's ratio	0.338	4.1
Tensile strength F_{11}^t , MPa	2352.3	3.76

3.2 TEN22

TEN22 tests are performed for determination of the tensile strength and the tensile modulus at 90° fibre alignment according with ASTM D3039-76.

The specimen lay up consists from 16 plies at 90°. The total thickness is equal to 2.0 mm and width of specimen is equal to 25 mm with consequently cross section area $A=50.0 \text{ mm}^2$. The specimens are 200 mm long and have brackets at the ends with thickness 1.5 mm and length 60.0 mm

Two strain gauges are applied, one in the longitudinal direction and second in the transverse direction.

The tensile modulus is at first calculated using a linear regression of the longitudinal stress-strain curve and then, according to the equation

$$E_2^t = \frac{\Delta P}{A \Delta \epsilon}$$

where ΔP is the load difference at the beginning and end of straight line part of the stress-strain curve, $\Delta \epsilon$ is a difference between strains at the same part of curve and A is the specimen cross section area. The tensile strength is calculated as ratio of the ultimate tensile load to the specimen cross sectional area A.

The mean values of the tensile modulus and the tensile strength are presented in Table 2. The standard deviations are also shown.

Table 2. TEN22 test mean values.

	Mean value	Standard deviation %
Tensile modulus E_2^1 , GPa	8.87	1.65
Tensile strength F_{22}^1 , MPa	47.28	10.6

3.3 TEN12

TEN12 tests are performed for determination of the in-plane shear modulus in axes 1 and 2 according with **ASTM D3518-76**.

The specimen lay up consists from 16 plies at 45° . The total thickness is equal 2.0 mm and width of specimen is equal 20 mm with consequently cross section area $A=40.0 \text{ mm}^2$. The specimens are 140 mm long and have brackets at the ends with thickness 1.5 mm and length 30.0 mm.

The direction at 45° has been applied due to using the same lay-up in the constructions manufactured from this material.

Two strain gauges are applied, one in the longitudinal direction and second in the transverse direction.

The shear modulus is at first calculated using a linear regression of the longitudinal stress-strain curve and then, according to the equation:

$$G_{12} = \frac{\Delta\tau_{12}}{\Delta\gamma}$$

where $\Delta\tau_{12}$ is the stress difference at the beginning and end of straight line part of stress-strain curve and $\Delta\gamma$ is a difference between the strains at the same part of curve. The shear stress is calculated by

$$\Delta\tau_{12} = \frac{\Delta P}{2A}$$

where ΔP is the load difference at the beginning and end of straight line part of stress-strain curve and A is the specimen cross section area. The shear strain $\Delta\gamma$ is calculated by

$$\Delta\gamma = \Delta\varepsilon_1 - \Delta\varepsilon_2$$

where $\Delta\varepsilon_1$ is a difference between strains in the direction 0° and $\Delta\varepsilon_2$ is a difference between strains in the direction 90° at the same part of curve. The mean value and standard deviation is presented in Table 3.

Table 3. In-plane shear modulus

	Mean value	Standard deviation %
In-plane shear modulus G_{12} , GPa	5.15	2.98

3.4 COM11

COM11 tests are performed for determination of the compression strength and the compression modulus at 0° fibre alignment according with **ASTM D3410-75**.

The specimen lay up consists from 48 plies at 0° . The total thickness is equal to 6.0 mm and width of specimen is equal to 15 mm with consequently cross sectional area $A=90.0 \text{ mm}^2$. The specimens are 76 mm long and have brackets at the ends with thickness 1.5 mm and a length 30.0 mm with a working zone 16 mm.



Fig. 2 A typical failure mode for compression

Two strain gauges are applied in the longitudinal direction from both sides. The compression modulus is at first calculated using a linear regression of the longitudinal stress-strain curve and then according to the equation

$$E_{11}^c = \frac{\Delta P}{A \Delta \epsilon}$$

where ΔP is the load difference at the beginning and end of straight line part of the stress-strain curve, $\Delta \epsilon$ is a difference between strains at the same part of curve and A is the specimen cross section area. The compression strength is calculated as ratio of the ultimate compression load and cross section area of the specimen. In Fig. 2a typical failure mode is shown in Fig. 2.

The standard deviations and mean values of the compression strength are presented in Table 4.

Table 4. COM11 test results

	Mean value	Standard deviation, %
Compression modulus E_{11}^c , GPa	142.6	2.3
Compression strength F_{11}^c , MPa	885.4	7.5

3.5 COM22

COM22 tests are performed for determination of the compression strength and the compression modulus for 90° fibre alignment according to **ASTM D3410-75**.

The specimen lay up consists of 48 plies at 0°. The total thickness is equal to 6.0 mm and width of specimen is equal to 15 mm with consequently cross sectional area $A=90.0 \text{ mm}^2$. The specimens are 76 mm long and have brackets at the ends with thickness 1.5 mm and length 30.0 mm with working zone 16 mm.

Two strain gauges are applied in the longitudinal direction of the specimen from both sides. The compression modulus is at first calculated using a linear regression of the longitudinal stress-strain curve and then according to the equation

$$E_2^c = \frac{\Delta P}{A \Delta \epsilon}$$

where ΔP is the load difference at the beginning and end of straight line part of the stress-strain curve, $\Delta \epsilon$ is a difference between strains at the same part of curve and A is the specimen cross section area. The compression strength is calculated as ratio of the ultimate compression load to the specimen cross sectional area. The mean values and standard deviations of the compression modulus and strength are presented in Table 5.

Table 5. Mean values for test COM22

	Mean value	Standard deviation, %
Compression modulus E_2^c , GPa	9.59	2.1
Compression strength F_{22}^c , MPa	233.2	4.8

3.6 COM12

COM12 tests are performed for determination the shear strength between axes 1 and 2 according to ASTM D4255/D4255M-94.

The specimen lay up consists from 16 plies at 0° . The total thickness is equal to 2.0 mm and width of specimen is equal to 60 mm with consequently cross sectional area $A=120.0 \text{ mm}^2$. The specimen geometry is shown in Fig. 3.

The ultimate stress is defines by equation

$$\tau_{12} = \frac{\max P}{A}$$

where max P is maximum load and A is the specimen cross sectional area. The mean value and standard deviation are presented in Table 6.

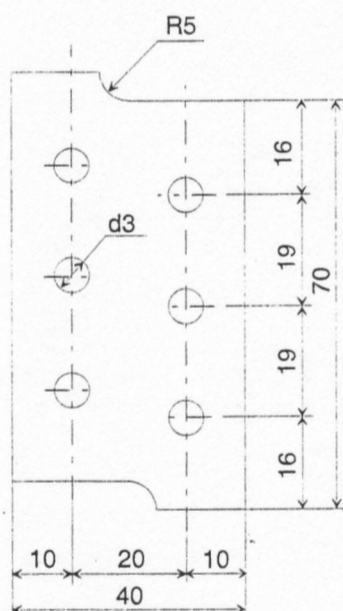


Fig. 3. Specimen for the test COM12

Table 6. Mean values for test TEN12

	Mean value	Standard deviation, %
Ultimate shear strength F_{12} , MPa	42	1.59

3.7 SHR11

SHR11 tests are performed for determination the interlaminar shear strength according to ASTM D2344-76.

The specimen lay up consists from 48 plies at 0°. The total thickness is equal to 6.0 mm and width of specimen is equal to 10 mm with consequently cross sectional area $A=60.0 \text{ mm}^2$. The loading device for specimen is shown in Fig. 4.

The ultimate stress is defined by equation

$$\tau_{13}^{\max} = F_{13} = \frac{0.75 \max P}{A}$$

where max P is maximal load at the test time. The mean value and standard deviation is presented in Table 7.

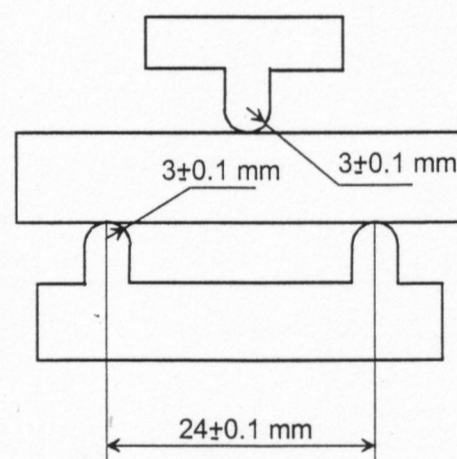


Fig. 4. Three point bending device for the SHR11 test

Table 7. Mean values for test SHR11

	Mean value	Standard deviation, %
Ultimate shear strength F_{13} , MPa	94.29	1.38

4 Summary of material properties obtained from static tests

Material properties of Unidirectional Tape Carbon/Epoxy material obtained from static tests based on ASTM guidelines are summarized in Table 8.

Table 8. Material properties from static tests

Modulus (GPa)					
E_1^t	E_1^c	E_2^t	E_2^c	G_{12}	ν_{12}^t
176	143	8.9	9.6	5.2	0.338
Strength (MPa)					
F_{11}^t	F_{11}^c	F_{22}^t	F_{22}^c	F_{12}	F_{13}
2352	885	47	233	42	94

This property is very sensitive on the specimen working zone length. Note that in RTU test the length of working zone for the test COM11 was 16 mm, but in IAI test the working zone was shorter.

5 Identification of elastic constants from vibration test

Conventional static tests are based on cutting samples from the composite plate. Such cutting can damage fibres and also small cracks can be introduced in the material. It can cause reduction of strength properties, especially transverse tension and in-plane shear strength.

A method based on identification of elastic constants from the measured frequencies of plate was previously used for glass/epoxy composites. The method was outlined in [4,5].

5.1 Experimental

Experiments were performed in Technion. The material manufactured was the same as used for the static tests. At all 7 unidirectionally reinforced composite plates (see Fig. 5) were tested. The plates were prepared with dimensions 200×200 mm and with the thickness 2 mm (16 plies) and 6 mm (48 plies). The actual density ρ of plates was measured. The plate is assumed to be a square plate ($a=b$), however actual dimensions are slightly different from the square. Note that thickness and density should be measured very accurate since these properties are used in the finite element model as input data and eigenfrequencies are rather sensitive to thickness and density of the plate.

The plate axes are noted as x , y and z and corresponding material axes are noted as 1, 2 and 3, where axis 1 is in the fibre direction axis 2 is in the transverse direction and axes 3 is in the thickness direction (see Fig. 5).

In the experiment the plates were hung on rubber threads in order to model the free-free (FFFF) boundary conditions on the edges. In the vibration experiment the eigenfrequencies and corresponding mode shapes were measured. The mode shapes are noted as (m, n) , where m is number of nodal lines parallel to the x axis and n is number of nodal lines parallel to y axis. For example, in Fig. 6 the mode shape $(1, 1)$ corresponding to the first experimental frequency $f_1=97$ Hz of the plate ud1 is presented. In Fig. 7 the mode shape $(2, 0)$ corresponding to the second frequency $f_2=123.8$ Hz of the plate ud1 is shown. In Fig. 7 the mode shape $(2, 1)$ corresponding to the third frequency $f_3=237.4$ Hz is presented. Similarly the experimental mode shapes were measured for other frequencies.

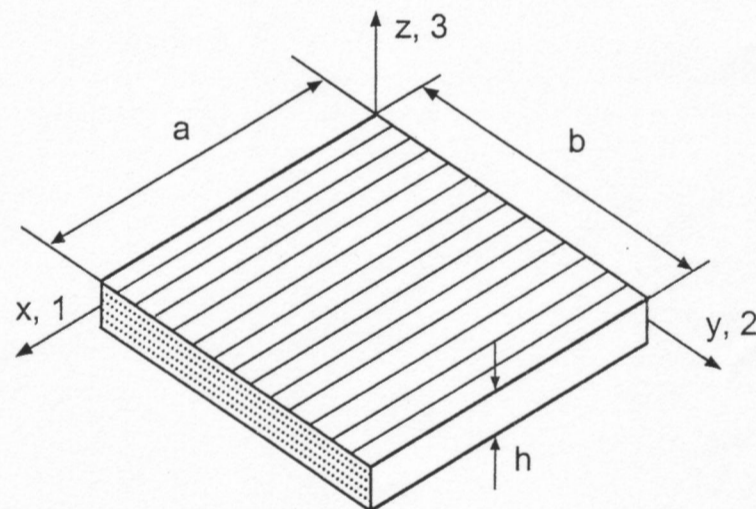


Fig. 5. Geometry of the composite plate

The experimentally measured frequencies and corresponding mode shapes for the plates ud1, ud2 and ud3 are presented in Table 9. Analysing the frequencies it is seen that for all plates experimental results are rather close. Note that for identification some selection of frequencies

can be performed. For identification of 5 elastic constants (plate is assumed to be a transversally isotropic material with 5 independent material parameters) at least 6 frequencies should be used [6]. For example, for the plate ud1 the third frequency is higher than for the plates ud1 and ud3. Such a difference may be due to some experimental error and it is not necessary to use this frequency in identification.

Table 9. Experimental frequencies and mode shapes for the plates ud1, ud2 and ud3

No.	ud1		ud2		ud3	
	Mode	f_i , Hz	Mode	f_i , Hz	Mode	f_i , Hz
1	(1,1)	97	(1,1)	97.6	(1,1)	98.2
2	(2,0)	123.8	(2,0)	123.4	(2,0)	126
3	(2,1)	237.4	(2,1)	245*	(2,1)	237
4	(3,0)	341	(3,0)	342	(3,0)	345.6
5	(3,1)	458	(3,1)	-	(3,1)	457
6	(0,2)	502.6	(0,2)	501	(0,2)	498
7	(1,2)	541.2	(1,2)	538	(1,2)	-
8	(2,2)	653	(2,2)	653	(2,2)	-
9	(4,0)	-	(4,0)	-	(4,0)	-
10	(4,1)	-	(4,1)	-	(4,1)	-
11	(3,2)	-	(3,2)	866	(3,2)	-
12	(5,0)	-	(5,0)	1124.5	(5,0)	-
13	(4,2)	1168	(4,2)	-	(4,2)	-
14	(5,1)	-	(5,1)	-	(5,1)	-
15	(0,3)	1381	(0,3)	-	(0,3)	-
16	(1,3)	1413	(1,3)	-	(1,3)	-
17	(2,3)	1512	(2,3)	-	(2,3)	-
18	(5,2)	-	(5,2)	1589	(5,2)	-

*this measurement could be not accurate



Fig. 6. Experimental mode shape (1, 1) for the first frequency of plate ud1

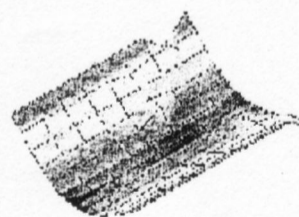


Fig. 7. Experimental mode shape (2, 0) for the second frequency of plate ud1

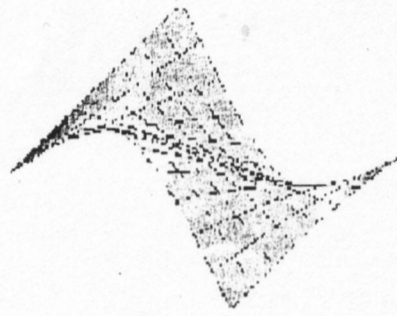


Fig. 8. Experimental mode shape (2, 1) for the third frequency of plate ud1

5.2 Identification functional

For identification the experiment design and response surface method (RSM) is employed together with the finite element modelling. The procedure of identification was outlined in [4,5] and here the so called first way of identification is employed. Thus, parameters of identification are five elastic constants of transversally isotropic material

$$E_1, E_2=E_3, G_{12}=G_{13}, \nu_{12}=\nu_{13}, G_{23}$$

Using the scaling of parameters the vector of identification parameters is given by [4,5]

$$\mathbf{x} = (x_1, x_2, x_3, x_4) = (\alpha_2, \alpha_3, \alpha_4, \alpha_4)$$

Here the parameters α_i are expressed through elastic constants [4,5].

The functional to be minimized describes deviation between the measured $\bar{\omega}_i = 2\pi f_i$ and numerically calculated $\omega_i(\mathbf{x})$ frequencies

$$\Phi(\mathbf{x}) = \sum_{i=2}^l \frac{(\bar{\omega}_i^2 - C\omega_i(\mathbf{x})^2)^2}{\bar{\omega}_i^4}$$

Numerical frequencies are calculated by the finite element method from the eigenvalue equation

$$\mathbf{K}(\mathbf{x})\mathbf{u} = \omega^2 \mathbf{M}\mathbf{u}$$

Here \mathbf{K} is a stiffness matrix, which depends on elastic constants and \mathbf{M} is a mass matrix. Solving this equation the frequencies and corresponding mode shapes can be obtained.

5.3 Experiment design and approximating functions

The experiment design with four variables and 35 reference points was selected. The initial guess value for the plate ud1 was assumed $E_1^0=171$ GPa, for ud2 the $E_1^0=171.6$ GPa, for ud3 the $E_1^0=171$ GPa.

Using the plans of experiment with 35 reference points for each plate in these reference points the finite element solution for about 20 first frequencies was obtained. Employing these numerical values of original functions the approximating functions (response surfaces) for all frequencies were obtained using the program RESINT [4,5]. For example, the approximating function (correlation $c=97.7\%$) for the third frequency of the plate ud1 is given by

$$f_3(\mathbf{x})=234.8-12.23*z_2-6.644*z_1-6.355*z_3$$

where normalized variables z_i were introduced

$$z_1 = -160.70+42.750*x_1$$

$$z_2 = -31.022+35.241*x_2$$

$$z_3 = -20.944+20.414*x_3$$

$$z_4 = -6.8635 + 23.324 \cdot x_4$$

Similar approximating functions were obtained also for other frequencies. These approximating functions are employed in identification functional instead of original functions (calculation by FEM). Minimization of identification functional has been performed employing the standard programs of constrained minimization in the MATLAB Optimisation Toolbox.

5.4 Results of identification and verification

Results of identification for all three plates are presented in Table 10. In the last column the mean values are presented. The values of Poisson's ratio are on the limits of domain of interest. Due to approximations an accuracy for the Poisson's ratio has been lost. It can be explained since this property is less sensitive to frequencies as modulus of elasticity. One possible way to obtain the Poisson's ratio is employing in minimisation the original (numerical) functions instead of approximating functions.

Table 10. Results of identification for plates ud1, ud2 and ud3

Property	ud1	ud2	ud3	Mean
E ₁ GPa	171.6	165	166.9	167.8
E ₂ GPa	10.45	10.07	10.61	10.38
G ₁₂ =G ₁₃ GPa	6.07	5.95	6.17	6.06
G ₂₃ GPa	6.24	6.47	5.97	6.23
ν ₁₂	0.42*	0.418*	0.227**	-

* upper limit of the preliminary selected domain of interest

** lower limit of the selected domain of interest

Verification of the results was performed by FEM calculating the residuals

$$\Delta_i = \frac{f_i^{FEM}(x^*) - f_i^{exp}}{f_i^{exp}} \times 100$$

Here x^* is vector of identified parameters.

Results of verification for the plate ud1 are shown in Table 11. For this plate at all nine frequencies marked with the sign (*) were used in identification. Three frequencies marked with the sign (#) are used for verification. It is seen that for all frequencies residuals are less than 1%. Even for frequencies (No. 8, 13 and 17), which were not used in identification residuals are very small.

Similar verification was performed for the plates ud2 and ud3. Note that for the plate ud2 in the identification at all 8 frequencies were taken into account, but for the plate ud3 only 6 frequencies were taken into account. Residuals also do not exceed 1%.

In Table 12 the elastic constants obtained by conventional static tests and employing the vibration tests and procedure of identification have been compared. In general good agreement is observed. The elastic modulus in fibre direction E₁ is in between the modulus in tension and compression. The transverse modulus E₂ and the in-plane shear modulus G₁₂ obtained in vibration test are higher than the values obtained in the static tests. It could be due viscoelasticity of the matrix since in vibration test the storage modulus is obtained, which always is higher than the static one.

Table 11. Experimental, numerical frequencies and residuals for the plate ud1.

No.	Mode	FEM (Hz)	Exp. (Hz)	Residuals Δ_1 (%)
1	(1,1)	97.9	97*	+0.92
2	(2,0)	123.9	123.8*	+0.08
3	(2,1)	235.6	237.4*	-0.75
4	(3,0)	341.2	341*	+0.06
5	(3,1)	454.9	458*	-0.68
6	(0,2)	503.4	502.6*	+0.16
7	(1,2)	540.8	541.2*	-0.07
8	(2,2)	651.4	653#	-0.25#
9	(4,0)	676.3	-	-
10	(4,1)	778.9	-	-
11	(3,2)	862.9	-	-
12	(5,0)	1111	-	-
13	(4,2)	1172	1168#	+0.34#
14	(5,1)	1214	-	-
15	(0,3)	1380	1381*	-0.07
16	(1,3)	1411	1413*	-0.14
17	(2,3)	1508	1512#	-0.26#

* these 9 frequencies were taken into account in identification functional

these 3 frequencies were used for verification only

Table 12. Comparison of elastic constants obtained from static and vibration tests

Property	Static test, RTU	Vibration test
E_1 GPa	176 (143)	167.8
E_2 GPa	8.9 (9.6)	10.38
$G_{12}=G_{13}$ GPa	5.2	6.06
G_{23} GPa	-	6.23
ν_{12}	0.338	-

Conclusion

The elastic properties were obtained employing two different methods – the conventional static tests according with the ASTM guidelines and vibration tests with procedure of identification. Results obtained by both methods are in good agreement. Strength properties were obtained by static tests only. Difference between strengths in direction 12 and 13 can be explained of the different methods for obtaining this results, technology of material manufacturing and conditions of the test processing.

References

1. Meier U., Kaiser H. Strengthening of structures with CFRP laminates // In: Proc. ASCE Conference on Advanced Composites Materials in Civil Engineering Structures, ASCE, New York, 1991 – p. 224-232.

2. Triantafyllou T.C., Deskovic N., Deuring M. Strengthening of concrete structures with prestressed fiber reinforced plastic sheets // In: ACI Structural Journal, Vol 89, N3, 1992 – p. 235-244.
3. Shahawy M.A., Beitelman T., Arockiasamy M., Sowrirajan Experimental investigation on structural repair and strengthening of damaged prestressed concrete slabs utilizing externally bonded carbon laminates // In: Composites: Part B vol. 27B, 1996 – p. 225-233
4. Rikards, R., Chate, A., Steinchen, W., Kessler, A. and Bledzki, A. K. Method for identification of elastic properties of laminates based on experiment design // In: Composites. Part B, **30**, 1999 - p. 279-289.
5. Rikards, R., Chate, A. and Gailis, G. Identification of elastic properties of laminates based on experiment design // In. Int. J. Solids and Structures, 2001 (in press).
6. Gagneja, S., Gibson, R. F. and Ayorinde, E. O. Design of test specimens for the determination of elastic through-thickness shear properties of thick composites from measured modal vibration frequencies // In. Comp. Sci. & Technol., Vol. 61, 2001 – p. 679-687.

Rolands Rikards

Rīgas Tehniskā Universitāte, Būvkonstrukciju Automatizētā projektsēšana,
LV-1658, Rīga, Kaļķu iela 1
Profesors, hab. Dr.sc.ing
E-pasts: rikards@latnet.lv

Aleksandrs Korjamins

Rīgas Tehniskā Universitāte, Būvkonstrukciju Automatizētā projektsēšana,
LV-1658, Rīga, Kaļķu iela 1
Docents, dr.sc.ing
E-pasts: aleks@latnet.lv

Andrejs Kovalevs

Rīgas Tehniskā Universitāte, Būvkonstrukciju Automatizētā projektsēšana,
LV-1658, Rīga, Kaļķu iela 1
Doktorants

Andris Čate

Rīgas Tehniskā Universitāte, Būvkonstrukciju Automatizētā projektsēšana,
LV-1658, Rīga, Kaļķu iela 1
Ass. Profesors, dr.sc.ing
E-pasts: and_cate@latnet.lv

Rikards R., Korjamins A., Kovalevs A., Čate A.

Vispārējo materiāla īpašību noteikšana izmantojot neliela izmēra paraugus

Daudzslāņaina materiāla īpašību novērtē, kas tiek armēts ar vienā virzienā klātu oglekļa šķiedru un slogots dažādos veidos, tiek izvērtēta šajā publikācijā. Materiāla elastīgās īpašības tika iegūtas izmantojot divas dažādas metodes – tradicionālo statistisko slogojuma pārbaudi, balstoties uz ASTM rekomendācijām, un vibrācijas pārbaudi ar identifikācijas procedūru. Abas šīs metodes deva līdzīgus iegūtos rezultātus. Stiprības īpašības tika noteiktas tikai ar statistiskām pārbaudēm.

Rikards R., Korjamins A., Kovalevs A., Čate A.

Characterization of material properties by means of small specimens

The characterizations of a unidirectional carbon fibre reinforced composite under the full range of in-plane loading conditions has been investigated. The elastic properties were obtained employing two different methods – the conventional static tests according with the ASTM guidelines and vibration tests with procedure of identification. Results obtained by both methods are in good agreement. Strength properties were obtained by static tests only.

Рикардс Р., Корякин А., Ковалев А., Чате А.

Исследование свойств материала, используя метод малых образцов

Исследованы характеристики однонаправленного многослойного композита армированного углеволокнами при различных условиях нагружения. Два метода были использованы для определения упругих свойств материала: метод статического тестирования в соответствии с рекомендациями Американских стандартов ASTM и метод идентификации по результатам вибрационного тестирования. Результаты, полученные обоими методами имеют хорошее совпадение. Прочностные характеристики определены только методом статического тестирования.

CO
CI
ŪI

J.R
De
J.S
De

Ats

Iev

Zer
tau
Pēc
dzī
ūde
kas
ka:

Šād
Šajā
radā

Ska

199
veid

199
kont
2170
veic
elek
Visu
"Kal